

Photocatalyzed Mineralization of Cresols in Aqueous Media with Irradiated Titania¹

RITA TERZIAN,* NICK SERPONE,*² CLAUDIO MINERO,† AND EZIO PELIZZETTI†‡

*Department of Chemistry, Concordia University, Montréal, Québec, Canada H3G 1M8; †Dipartimento di Chimica Analitica, Università di Torino, Torino, Italy 10125; and ‡Dipartimento di Chimica Fisica Applicata, Università di Parma, Parma, Italy

Received March 6, 1990; revised August 22, 1990

Titania, TiO₂, irradiated by ultraviolet/visible light was used to mediate the photocatalyzed degradation of *ortho*-cresol, *meta*-cresol, and *para*-cresol. The total photomineralization of these phenols to carbon dioxide and water occurs in air-equilibrated aqueous media. Two major hydroxylated aromatic intermediate species have been identified by liquid chromatographic methods: 4-methylcatechol and methylhydroquinone. Photochemical efficiencies (lower limits of quantum yields, 365 nm) of compound disappearance are, respectively, 0.0096, 0.0076, and 0.010 for *o*-, *m*-, and *p*-cresol. The effect of such parameters as pH, initial cresol concentration, and radiant power levels on the degradation of *m*-cresol was examined in detail. Although the photodegradation process kinetics show similarities with Langmuir-Hinshelwood-type behavior, namely saturation, it is shown that the resulting kinetic expression for the rate of degradation is a complicated function of various parameters and is silent as to the details of the initial photooxidative steps. It is implicitly argued, however, that the reaction takes place on the semiconductor particle surface. © 1991 Academic Press, Inc.

INTRODUCTION

Contamination of water resources by a variety of organic substances is an increasingly common problem in industrialized areas. Nine general classes of environmental contaminants have been identified (1) that include the cresols. Common uses of these phenolic substrates range from fumigants and insecticides to wood preservatives and disinfectants (2, 3).

In the past several years we have surveyed the photocatalyzed destruction (mineralization) of a number of organics, members of the United States Environmental Protection Agency's list of top priority pollutants (1), using titania (Degussa P-25 TiO₂) under ultraviolet/visible or simulated sun-

light irradiation. In each instance, total mineralization was demonstrated by following the temporal evolution of the products CO₂ and H₂O (or HCl for chloroorganics) along with the concomitant disappearance of the original substrate. Recently, we have begun systematic kinetic studies on TiO₂ mediated photooxidations on some of the environmental organic and inorganic pollutants (4-6). Herein, we examine specifically the temporal course of the mineralization of three cresols (*ortho*-, *meta*-, and *para*-cresol) in air-equilibrated (or oxygen-saturated) TiO₂ suspensions. We report the effect(s) of such parameters as pH, initial cresol concentration, and radiant power levels of the light source. Photochemical efficiencies, which represent lower limits of the true quantum yields, for the disappearance of the cresol at the irradiation wavelength of 365 nm (bandpass ±10 nm) have also been determined. Some hydroxylated aromatic intermediates have been identified and rate

¹ Part 5 of "Kinetic Studies in Heterogeneous Photocatalysis."

² To whom correspondence should be addressed.

data are presented in the context of kinetic expressions borrowed from enzyme-type behavior (7).

EXPERIMENTAL

Materials

o-, *m*-, and *p*-Cresol, methylhydroquinone, 4- and 3-methylcatechol, 2-methylresorcinol, and orcinol monohydrate (3-methylresorcinol) (Aldrich, $\geq 99\%$ pure) were used as supplied without further treatment. Titanium dioxide was Degussa P-25 (BET surface area, 55 m²/g; mostly in the anatase form and consisting of 99.5% TiO₂, and <0.3% Al₂O₃, <0.3% HCl, <0.2% SiO₂ and <0.01% Fe₂O₃ as impurities some of which are probably segregated on the particle surface) (8). Water was doubly distilled throughout. The mobile phase used for the HPLC analyses consisted of a mixture (see below) of methanol (BDH, omnisolv grade), doubly distilled water, and *ortho*-phosphoric acid (Fisher, HPLC grade).

Procedures

Irradiation at wavelengths ≥ 300 nm was carried out on 50-ml samples (unless otherwise noted) contained in Pyrex glass reactors. The temperature during the course of the reaction was $30 \pm 2^\circ\text{C}$. The appropriate quantity of a stock solution of the cresol was added to a previously weighed amount of TiO₂ (unless otherwise stated, 100 mg to give a 2-g/liter catalyst loading). The pH of the stock solutions was adjusted with HCl (pH 3) or with NaOH (pH 12). For studies at pH 12, the aliquots were acidified prior to analysis.

The light source was a 1000 Hg/Xe lamp operated at ca. 900 W; it was equipped with a water jacket to filter out infrared radiation. The radiant power level dependence of the mineralization process was performed using appropriate neutral density filters in the light path.

Where CO₂ evolution was monitored, 25-ml solutions were used; the flasks were sealed with rubber septa and aluminum seals. For *m*-cresol, the degradation was

also carried out in an oxygen-saturated atmosphere; the flask was oxygen purged for about 10 min. Typically, the temporal course of the mineralization was sampled at ca. 30-min intervals. The flask was removed from the irradiation source, and a suitable aliquot (about 2 ml) was taken; subsequently, the flask was once again purged with oxygen for 5 min followed by continued irradiation.

Photochemical efficiencies were determined at 365 nm (Bausch & Lomb monochromator; bandpass, ± 10 nm). The radiant power (mW/cm²) of the light source for both photochemical efficiency and radiant power level dependence experiments was ascertained with a calibrated power meter (Laser Instrumentation Ltd., Model 154BT).

Analyses

The temporal evolution of the mineralization of the cresols and identification of the respective reaction intermediates were monitored by high performance liquid chromatographic (HPLC) techniques using a Waters Associates liquid chromatograph equipped with a 501 HPLC pump, a 441 absorbance detector, and a Hewlett-Packard 3396A integrator. The detection wavelengths were 214 nm (Zn lamp) and 280 nm (Hg lamp). The column was a Whatman reverse phase C-18 (Partisil-10, ODS-3). The mobile phase consisted of a mixture of methanol/water/*o*-phosphoric acid (in a 40/59.9/0.1 or a 25/74.9/0.1 ratio). The latter afforded a better separation of the HPLC signals and facilitated identification of the intermediates. The flow rate was 2 ml/min. The aliquots from the reaction slurry were centrifuged (1000 rpm) for about 5 min and subsequently filtered through an MSI nylon 66 filter (pore size, 0.22 μm) prior to analysis. When needed, UV/visible absorption and/or diffuse reflectance spectra were taken on a Shimadzu 265 SP UV/vis spectrophotometer.

Carbon dioxide evolution was monitored by gas chromatographic methods using a GOW-MAC gas chromatograph equipped

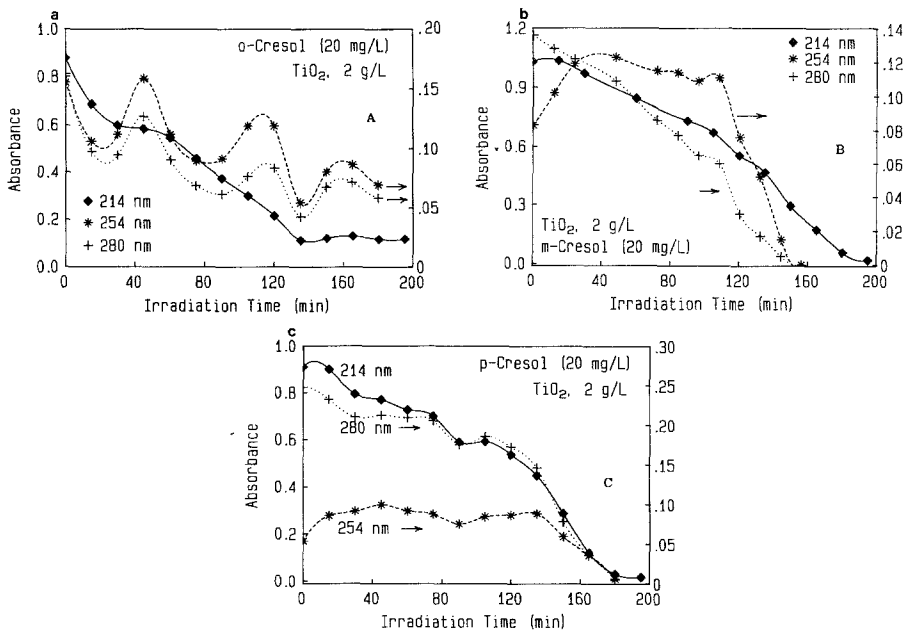


FIG. 1. Absorbance versus irradiation time plots at three monitoring wavelengths relevant to the HPLC technique employed in this work (214, 254, and 280 nm) in the mineralization of 20 mg/liter of cresols in the presence of 2 g/liter TiO_2 at pH 3: (a) *o*-cresol, (b) *m*-cresol, and (c) *p*-cresol.

with a Porapak-N column. Helium was the carrier gas. The GC had been calibrated previously as follows: known amounts of Na_2CO_3 were added to a 2 g/liter suspension of TiO_2 in water; the flask was sealed and an appropriate quantity of HCl was added to bring the pH to 3. Subsequently, the sample was irradiated for 1 hr following which the gases in the headspace volume were sampled and injected into the chromatograph. For *p*-cresol, the complete mineralization was also verified by the quantitative determination of CO_2 using the BaCO_3 test after the complete disappearance of the reactant substrate.

RESULTS AND DISCUSSION

The UV absorption spectra of the three cresols in aqueous media, examined in this work, show strong spectral similarities. In particular, the spectra of *o*- and *m*-cresol are identical with absorption bands at 213, 270, and 277 nm; the corresponding bands for *p*-cresol are red-shifted by ca. 7 nm. There is

thus an inherent difficulty in distinguishing between the three cresols on spectral considerations alone. Monitoring the degradation of these substrates by UV spectral methods at various wavelengths (214, 254, and 280 nm) is not facilitated as illustrated in Figs. 1a-c, which show plots of absorbance vs irradiation time. For *m*- and *p*-cresol, the plots tend to zero absorption after about 2.5–3.5 hr of irradiating the TiO_2 suspensions. This was not the case for *o*-cresol (Fig. 1a). There probably exists some longer lived intermediate for this species even after ca. 3 hr of irradiation at the monitored wavelengths. The erratic behavior of the plots, which arises from the evolution and disappearance of intermediates with similar but not identical spectral properties at different times along the course of the reaction, precluded the spectral method as an analytical tool.

Catalyst loading in the light-induced splitting of H_2S (9), in photooxidation of organics (10), or in the photoreduction of trace

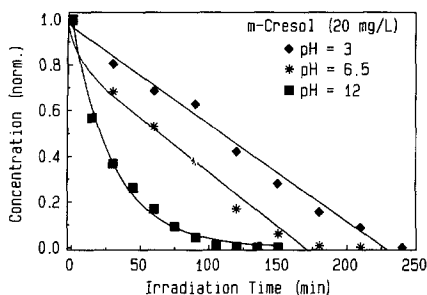
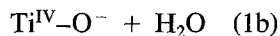
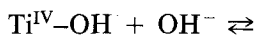
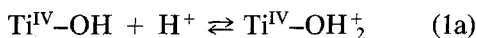


FIG. 2. Plots of the normalized concentration as a function of irradiation time for the photomineralization of *m*-cresol (20 mg/liter) at three different pH's: 3, ~6.5, and 12; concentration of TiO_2 , 2 g/liter.

metals from dilute solutions (11) has often been 2g/liter of the semiconductor material (TiO_2 , CdS, ZnO, and others). In the present instances, the initial rate of degradation of *m*-cresol (169 μM ; ca. 20 mg/liter) showed little change with variations in the concentration of TiO_2 between 0.1 and 4 g/liter. A catalyst loading of 2 g/liter is equally appropriate under our conditions; this loading was subsequently used throughout.

Another parameter of some import in reactions taking place or involving semiconductor particle surfaces in heterogeneous media is the pH of the suspensions, as it often dictates the surface characteristics of the catalyst. For the TiO_2 material used in this work, the zero zeta potential occurs at pH ~5.6. At more acidic pH the semiconductor particle surface is positively charged, while at pH > 5.6 the surface is negatively charged (reaction (1)):



This bears important consequences on the adsorption/desorption properties of the catalyst's particle surface, as well as, no doubt, on the photoadsorption/photodesorption features of such surfaces. The influence, therefore, that pH changes will have on interfacial electron transfer kinetics (photoreductions and photooxidations) is evident (12). Figure 2 illustrates the temporal course

of the photodegradation of *m*-cresol (20 mg/L) at three pH's (pH 3, pH ~ 6.5, and pH 12). Clearly, degradation is most rapid in alkaline media where the phenoxide species is present (pK of cresols ≈ 10 (13)) and slowest at pH 3. The quantitative aspects of the photodegradation process are treated later. While alkaline media might seem most suited to carry out the photomineralization of organic contaminants, we deliberately chose to investigate the process in acidic media (henceforth, pH 3) to avoid the possible occurrence of direct photolysis, as witnessed in our earlier study on the photocatalyzed mineralization of 4-chlorophenol (14) and pentachlorophenol (15).

Identification of Intermediates

At an initial pH of 3 and with the mobile phase used (25/74.9/0.1 in methanol/water/*o*-phosphoric acid), the HPLC chromatograms showed only two clearly detectable intermediates formed for each of the three cresols examined. Table 1 summarizes the retention times (r.t., min) of the cresols and the intermediates denoted as 1, 2, A, and B. The species that can form by monohydroxylation (see below), as well as the corresponding retention time of each species, determined from originally pure substrates (except for 4-methylresorcinol) under iden-

TABLE 1

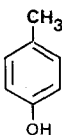
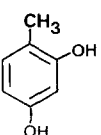
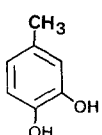
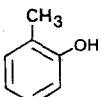
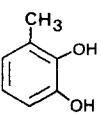
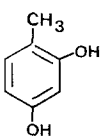
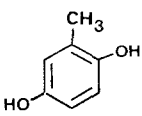
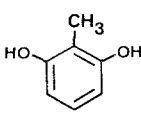
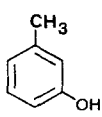
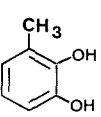
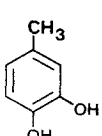
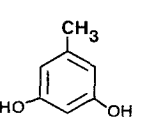
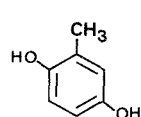
HPLC Retention Times of Intermediates Produced from the Photodegradation of Cresols in Air-Equilibrated TiO_2 Aqueous Suspensions (20 mg/liter in cresol; pH 3).^a

Intermediate:	1	2	A	B
Retention times:	3.8 min	7.3 min	4.6 min	3.45 min
<i>o</i> -Cresol (14.1 min)	✓	—	✓	—
<i>p</i> -Cresol (14.5 min)	—	✓	—	✓
<i>m</i> -Cresol (14.1 min)	✓	✓	—	—

^a Mobile phase: 25:74.9:0.1; MeOH, water, *o*- H_3PO_4 .

TABLE 2

Identification of Intermediates Produced in the Photomineralization of Cresols in Air-equilibrated TiO₂ Aqueous Suspensions (pH; 3; 20 mg/liter in Cresol)—Values in Parentheses Denote Retention Times

Cresol	Potential Intermediates (dihydroxytoluenes)				
 p-Cresol (14.5 min)	 4-Methylresorcinol (3.45 min)	 4-Methylcatechol (7.3 min)			
 o-Cresol (14.1 min)	 3-Methylcatechol (7.9 min)	 4-Methylresorcinol (3.45 min)	 Methylhydroquinone (3.8 min)	 2-Methylresorcinol (4.0 min)	
 m-Cresol (14.1 min)	 3-Methylcatechol (7.9 min)	 4-Methylcatechol (7.3 min)	 Orcinol (5.6 min)	 Methylhydroquinone (3.8 min)	

tical experimental conditions, are shown in Table 2. Comparison of these r.t. aided considerably in identifying the intermediates formed.

Hydroxylation of *p*-cresol yields two intermediates: 4-methylresorcinol and 4-methylcatechol. By contrast, both *o*- and *m*-cresol can in principle yield four isomeric species. Comparing the retention times of Table 2 with those from the liquid chromatograms indicates that species 2 (r.t. 7.3 min), common to both the *p*- and *m*-cresol, is 4-methylcatechol (4-MCC). The common intermediate 1 with r.t. at 3.8 min in *o*- and *m*-cresol is identified with methylhydroquinone (MHQ). The intermediate B with r.t. 3.45 min, seen in the reaction of *p*-cresol, is tentatively ascribed to 4-methylresorcinol; understandably, this species does not appear in the degradation of *o*-cresol as hy-

droxylation would have to occur at position meta to the OH substituent on the toluene moiety. The identity of species A (Table 1 for *o*-cresol) with r.t. of 4.6 min is enigmatic. It is neither 2-methylresorcinol (r.t. 4.0 min) nor 3-methylcatechol (r.t. 7.9 min), which also does not form from *m*-cresol. It is not unlikely that the quantities of these species are such that they were undetectable under our conditions. We cannot rule out methylbenzoquinone or a possible trihydroxytoluene species for A; trihydroxylated benzene intermediates have been reported in the photomineralization of phenol but in very small quantities (0.3% pyrogallol and 2.1% hydroxyhydroquinone) (16, 17).

Formation of 4-methylcatechol in the degradation of the cresols is confirmed by the diffuse reflectance spectra (Fig. 3) taken on the catalytic powder after filtration of the

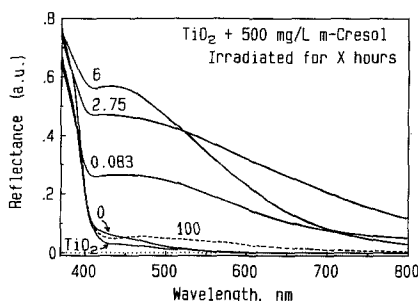


FIG. 3. Diffuse reflectance spectra of the catalyst powder from an air-equilibrated aqueous suspension of TiO_2 (2 g/liter) and 500 mg/liter of *m*-cresol after several hours of irradiation.

samples (TiO_2 and 500 mg/liter *m*-cresol) taken at various time intervals from the radiation source. Before irradiation but after equilibration of the suspension in the dark, comparison of the spectral features at ~ 420 –500 nm with those for TiO_2 alone shows that some of the *m*-cresol is physisorbed on the semiconductor particle surface. After 5 min of irradiation, the spectra show a strong feature over the whole spectral range examined (400–800 nm); the feature grows to 6 hr of irradiation. The TiO_2 catalyst powder appears grayish-pink coloured at this point. Identical spectral features were observed from a suspension consisting of TiO_2 and pure 4-methylcatechol (18). Continued irradiation leads to a significant decrease in the intensity of the reflectance spectrum (100 hr) which approaches that of TiO_2 ; it is also accompanied by a significant discoloration of the catalytic powder.

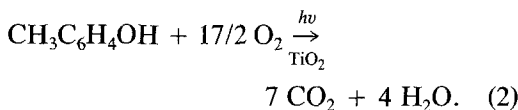
Degradation of Cresols

None of the cresols investigated here undergo changes in the dark in the presence of TiO_2 . Any degradation of these substrates is therefore the result of light-induced processes. Direct irradiation of aqueous solutions of the cresols with ultraviolet/visible light, but in the absence of the semiconductor catalyst, leads to very small decreases

in [cresol]: 3 to 5% after ~ 6 hr of irradiation (see Figs. 4a–c). For 20 mg/liter of the cresols, the apparent rate constants are $6.3 \times 10^{-5} \text{ min}^{-1}$ (*o*-cresol), $18 \times 10^{-5} \text{ min}^{-1}$ (*m*-cresol), and $9.9 \times 10^{-5} \text{ min}^{-1}$ (*p*-cresol), about 1 to 2 orders of magnitude smaller than the catalyzed processes (0.4 – $1.3 \times 10^{-2} \text{ min}^{-1}$; see below).

The photocatalyzed decomposition of the three cresols in the presence of TiO_2 is presented in Figs. 4a–c. Both *o*- and *p*-cresol (20 mg/liter) degrade via first-order kinetics. Curiously, *m*-cresol (also 20 mg/liter) appears to decompose by zero-order kinetics under identical experimental conditions of light source and initial pH. The formation and subsequent degradation of the two intermediates detected are also indicated. In each case, total disappearance of the original cresol and decomposition of the intermediate species occur in ≤ 4 hr of irradiation. The corresponding apparent rate constants (first-order or pseudo first-order), initial rates, and half-lives for the degradation of the three cresols as a function of initial [cresol], pH, and in the presence of excess oxygen for *m*-cresol are summarized in Table 3. The apparent kinetic parameters for the intermediates are collected in Table 4.

The photocatalyzed mineralization process follows the stoichiometric reaction (2), as evidenced by a quantitative product analysis:



The quantity of CO_2 evolved as a function of irradiation time is illustrated in Fig. 5. Approximately $32.5 \mu\text{mol}$ of CO_2 were expected from reaction 2 for an initial [cresol] of 20 mg/liter. It is evident that after ~ 4 hr of irradiation, when all the cresols and the aromatic intermediate species have decomposed, only about 65–70% of CO_2 is produced; 80–85% of CO_2 is evolved after about 7 hr of irradiation. We infer that other inter-

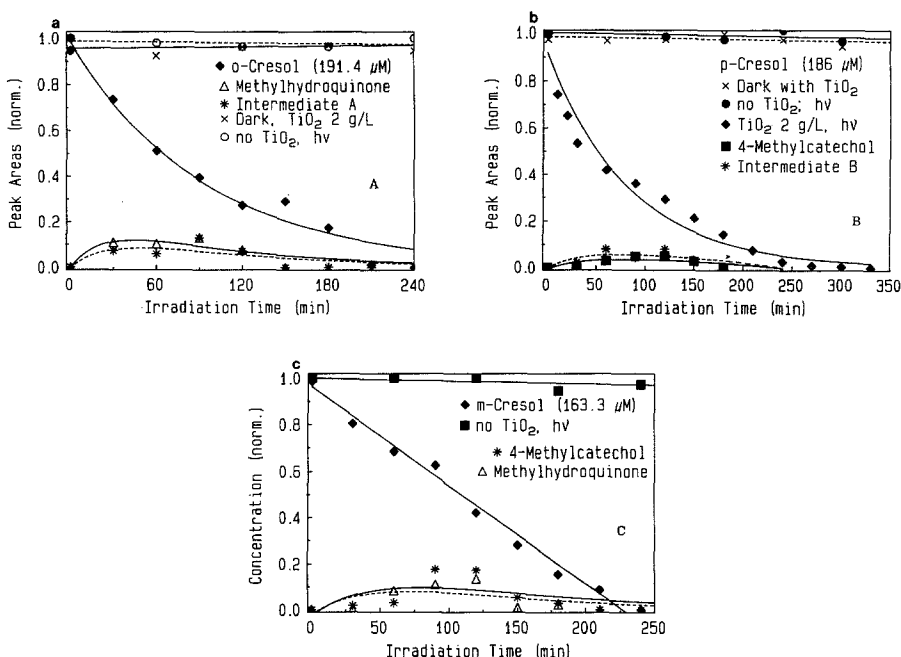


FIG. 4. Plots of normalized peak areas (or concentration) as a function of irradiation time showing the degradation of the three cresols (ca. 20 mg/liter) and formation and decomposition of two intermediates in the photomineralization process with irradiated TiO_2 present (2 g/liter) at pH 3. The behavior of the cresols under dark conditions but in the presence of the TiO_2 , and under direct photolysis (no TiO_2 present), is also indicated: (a) *o*-cresol, (b) *p*-cresol, and (c) *m*-cresol. The curves are computer fits to equations noted in the text.

TABLE 3

Apparent Kinetics of the Mineralization of Cresols Photocatalyzed by Irradiated TiO_2 in Air-Equilibrated Suspensions at $\text{pH}_i \sim 3$

Cresol	[Cresol] (μM)	k_{app} (10^{-3} min^{-1})	Initial rates ($\mu\text{M min}^{-1}$)	$t_{1/2}(\text{app})$ (min)
<i>o</i> -Cresol	185	11.2 \pm 1.0	2.07 \pm 0.18	62 \pm 6
	191	10.5 \pm 0.8	2.01 \pm 0.16	66 \pm 5
<i>p</i> -Cresol	186	12.0 \pm 1.1	2.23 \pm 0.20	58 \pm 5
	194	13.9 \pm 1.0	2.69 \pm 0.20	50 \pm 4
<i>m</i> -Cresol	2.03	86.2 \pm 7.7	0.175 \pm 0.016	8.0 \pm 0.7
	17.1	22.8 \pm 2.8	0.390 \pm 0.047	30 \pm 4
	185	3.98 \pm 0.17	0.736 \pm 0.031	174 \pm 7
	163	4.25 \pm 0.16	0.694 \pm 0.026	163 \pm 6
	443	2.12 \pm 0.08	0.993 \pm 0.035	327 \pm 12
	905	1.10 \pm 0.05	0.996 \pm 0.048	630 \pm 29
	4966	0.154 \pm 0.008	0.765 \pm 0.040	4500 \pm 234
	186 ^a	11.8 \pm 0.6	2.19 \pm 0.11	59 \pm 3
176 ^b	4.76 \pm 0.38	0.836 \pm 0.067	146 \pm 12	
164 ^c	31.3 \pm 1.2	5.13 \pm 0.19	22 \pm 1	

^a In oxygen-saturated suspensions.

^b $\text{pH}_i \sim 6.5$.

^c $\text{pH}_i \sim 12$.

TABLE 4

Apparent Kinetics in the Formation of Intermediates Produced at pH_i 3 in Air-Equilibrated Irradiated TiO₂ Suspensions

Parameter	Source		
	<i>o</i> -Cresol	<i>p</i> -Cresol	<i>m</i> -Cresol
[Cresol], μM	191	186	163
k_{app} (degradation), min^{-1}	0.0105	0.012	0.0043 (.0118) ^a
k_{app} (formation), min^{-1}			
4-MCC	—	0.014	0.0043
MHQ	0.011	—	0.0043
Interm.	0.011 (A)	0.014 (B)	—
k_{app} (degradation), min^{-1}			
4-MCC	—	0.014	0.02
MHQ	0.04	—	0.03
Interm.	0.03 (A)	0.014 (B)	—
k_{app} (CO ₂ formation), min^{-1}	~0.0076	~0.012	~0.0095 (0.032) ^a

^a In an oxygen-saturated suspension.

mediates (aliphatic) are formed which are slow to degrade. Possibly, the suspension may be starved of needed oxygen (14).

The effect of the oxygen concentration on the kinetics of decomposition of *m*-cresol was determined by carrying out the mineralization process under conditions where the suspension was always saturated with molecular O₂. The decomposition of this cresol in air-equilibrated and in oxygen-saturated suspensions is compared in Fig. 6a. Apparent zero-order kinetics are also evident for the latter. The corresponding parameters

are air vs. O₂, respectively k_{app} , 3.98×10^{-3} and $11.8 \times 10^{-3} \text{ min}^{-1}$; initial rates, 0.74 and $2.2 \mu M/\text{min}$; $t_{1/2}(\text{app})$, 174 and 59 min. Note that in the presence of excess oxygen, decomposition of *m*-cresol occurs in <1.5 hr. Comparison of the evolution of carbon dioxide from air-equilibrated and oxygen-saturated suspensions is made in Fig. 6b. For the latter suspensions, approximately 60% of CO₂ evolved after the cresol had decomposed. Near quantitative formation of CO₂ occurred in ca. 2.5 hr; $k_{app} \sim 9.5 \times 10^{-3} \text{ min}^{-1}$ (air) and $32 \times 10^{-3} \text{ min}^{-1}$ (O₂). The slower evolution of products cannot be due solely to the lack of oxygen, but rather to the intermediacy of the aliphatic intermediates.

pH Dependence

m-Cresol was chosen for more detailed investigation into the effect of pH on the total degradation to CO₂ and water. Air-equilibrated aqueous TiO₂ suspensions of 20 mg/liter of this substrate were examined at pH 3, at pH ~ 6.5, and at pH 12 (0.01 M NaOH). The respective k_{app} are 3.98×10^{-3} , 4.76×10^{-3} , and $31.3 \times 10^{-3} \text{ min}^{-1}$. The photomineralization in alkaline media follows first-order kinetics, unlike that in acidic

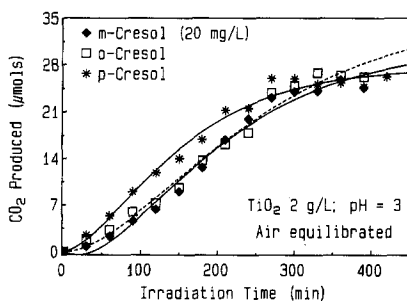


FIG. 5. Plots showing the temporal evolution of CO₂ from the photomineralization of 20 mg/liter cresol in the presence of 2 g/liter TiO₂ at an initial pH of 3; air-equilibrated suspensions.

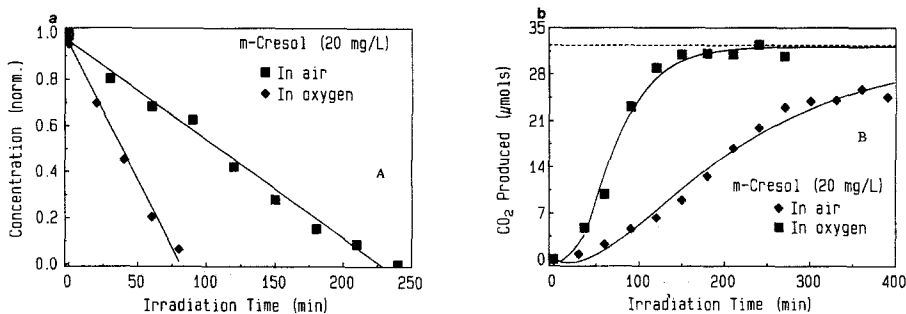


FIG. 6. (a) Plots showing the photodegradation of 20 mg/liter of *m*-cresol in the presence of 2 g/liter TiO₂ in air-equilibrated suspensions and in oxygen-saturated suspensions; initial pH 3. (b) Plots showing the corresponding temporal evolution of CO₂ from the photomineralization of 20 mg/liter of *m*-cresol in air-equilibrated and oxygen-saturated suspensions of TiO₂.

media. This results because adsorption requires interaction between two negatively charged entities at pH 12 (the negative particle surface and the phenoxide), thereby leading to low surface coverage at this pH and concentration of *m*-cresol. Figure 7 depicts, as normalized peak heights versus irradiation time, the temporal course of the degradation of *m*-cresol at pH 12 in the absence (direct photolysis) and presence of TiO₂. Direct photolysis proceeds via zero-order kinetics; the pseudo first-order k_{app} ($17 \times 10^{-5} \text{ min}^{-1}$) is similar to that from the direct photolysis at pH 3, but is about 20 times slower than for the catalyzed process.

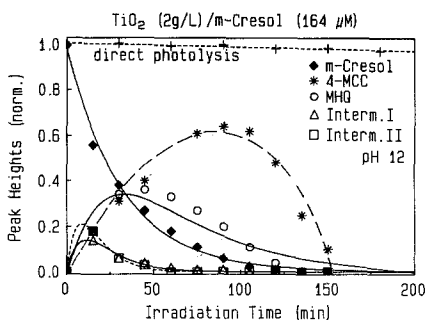


FIG. 7. Photodegradation of 164 μM *m*-cresol via direct photolysis and via the photocatalyzed process in the presence of TiO₂ at an initial pH of 12. Also shown are the formation and subsequent degradation of the four intermediate species detected by HPLC methods (see text).

Four intermediates were detected at pH 12: 4-methylcatechol, methylhydroquinone, and two unidentified intermediates (I and II). The corresponding apparent first-order rate constants for both formation and degradation of these species are 0.029 and 0.030 min⁻¹ (MHQ), 0.086 and 0.087 min⁻¹ (I), and 0.113 and 0.114 min⁻¹ (II). 4-Methylcatechol forms via first-order kinetics ($4.7 \times 10^{-4} \text{ min}^{-1}$); it degrades via a zero-order process (pseudo first-order $k_{app} \sim 0.41 \text{ min}^{-1}$).

Concentration Dependence

The photomineralization of *m*-cresol occurs via zero-order kinetics (Fig. 8a,b and Table 3) for all concentrations examined {0.2 mg/liter ($2.03 \mu\text{M}$) to 500 mg/liter ($4966 \mu\text{M}$)}; the rate constants vary from 0.175 to $0.996 \mu\text{M}/\text{min}$. A plot of initial rates of photodegradation (R_{in}) vs. initial [*m*-cresol] reveals similarities with Langmuir-Hinshelwood (LH) type behavior Fig. 9a): $R_{in} = k'_{app} K [m\text{-cresol}] / (1 + K [m\text{-cresol}])$ (7). The linear transform of this expression (Fig. 9b) yields the zero-order $k'_{app} = 0.86 \pm 0.06 \mu\text{M}/\text{min}$ and $K = 4.8 \pm 0.6 \times 10^{-4} \text{ M}^{-1}$.

Radiant Power Level Dependence

The dependence of the photodegradation of *m*-cresol (20 mg/liter) on the radiant power level of the light source is illustrated in Fig. 10. The initial rate increases linearly

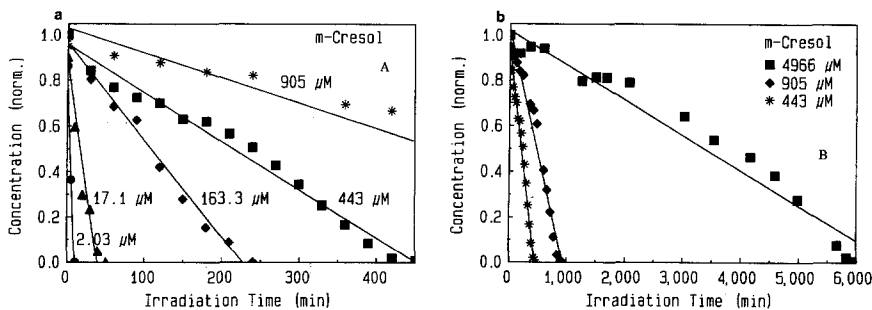


FIG. 8. Zero-order plots of the photomineralization of *m*-cresol catalyzed by irradiated TiO_2 at various initial concentrations; initial pH 3.

(slope = $0.029 \pm 0.002 \mu\text{M cm}^2/\text{mW min}$) with power level (low light fluxes) suggesting that electron/hole recombination is not the sole major deactivating pathway for photogenerated electrons and holes; the photooxidative step(s) on the semiconductor catalyst can also compete effectively as demonstrated by the very fact that photodegradation of the substrates does occur, albeit at low photochemical efficiencies (see below).

Photochemical Efficiencies

Owing to the bandgap of 3.2 eV of the semiconductor used (TiO_2), only light radiation of wavelengths below 400 nm can drive the photocatalyzed process. The quantum efficiencies for the decomposition of the cresols were determined at 365 nm (bandpass ~ 20 nm) and reflect the number of mole-

cules of the cresol that degrade per incident photon: 0.0096 (*o*-cresol), 0.0076 (*m*-cresol), and 0.010 (*p*-cresol).

Reactive Species

Much of the available evidence reported thus far points to the OH radical as the principal species in the photomineralization of numerous organic substrates (19–22). The observation made herein of hydroxylated intermediate products (4-MCC and MHQ) as well as similar species in the photooxidation of phenol (4, 16, 17), is evidence that $\cdot\text{OH}$ is the primary reactive species. Studies on the photooxidation of isopropanol in TiO_2 and ZnO suspensions have inferred that the rate of formation of the $\cdot\text{OH}$ radical is rate determining (23). As well, electron paramagnetic resonance investigations by spin trapping methods have identified the $\cdot\text{OH}$

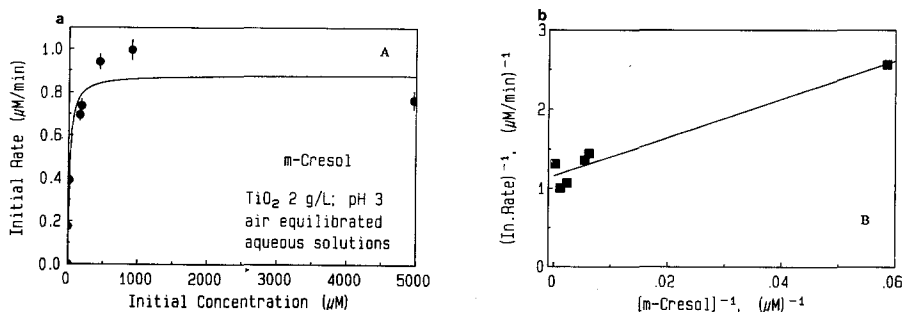


FIG. 9. (a) Plot showing the effect of the initial concentration on the initial rate of the photodegradation of *m*-cresol under air-equilibrated conditions; initial pH 3. (b) Linear transform of the Langmuir-type isotherm (see text).

k_{7b} to represent the sum of microrate constants $\sum_i k_{A_i}$ and $\sum_j k_{B_{i,j}}$, respectively, the concentrations of A , B_i , and $C_{i,j}$ at some time t will be given by (31)

$$[A(t)] = [A]_0 \exp\{-k_{7a}t\} \quad (8)$$

$$[B_i(t)] = \{k_{7a}[A]_0/(k_{7b} - k_{7a})\} \{\exp(-k_{7a}t) - \exp(-k_{7b}t)\} \quad (9)$$

and

$$[C_{i,j}(t)] = \{[A]_0/(k_{7b} - k_{7a})\} \{k_{7b}(1 - \exp(-k_{7b}t)) - k_{7a}(1 - \exp(-k_{7a}t))\} \quad (10)$$

for first-order processes. For a zero-order process (32)

$$[A(t)]/[A]_0 = 1 - k_{app}t. \quad (11)$$

The data in Figs. 2 and 4–8 were curve-fitted using the above expressions; values of k_{7a} and k_{7b} are collected in Table 3 for the photomineralization of all three cresols.

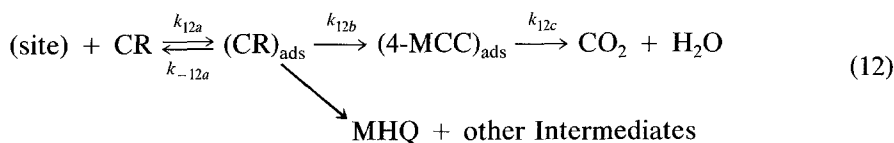
Kinetic Considerations

We have mentioned earlier that photooxidations of the cresols in a heterogeneous medium occur by reaction between an OH radical and the cresol as a first step. If the process occurred between a surface-adsorbed species and a bulk solution substrate, it would follow the Eley–Rideal (ER) pathway. By contrast, if both the reacting species were adsorbed on the semiconduc-

tor particle surface, the process would then follow the Langmuir–Hinshelwood (LH) route (33). For the latter, the two species may be adsorbed on the same sites competitively or they may be adsorbed on different surface sites. The LH pathway predominates in several photooxidative conversions (34); some examples where the ER and the LH routes both contribute to the overall transformations have been documented (34).

Adsorption and/or photoadsorption can occur on two identifiable surface sites: Ti^{III} sites and $Ti^{IV}-OH^-$ sites. Organic substrates adsorb on surface hydroxyls (35) while molecular O_2 adsorbs onto the Ti^{III} sites (36) from whence the superoxide radical forms (37).

Although the cresols are only adsorbed to a slight extent (<5% in the dark) on TiO_2 particles, the extent of *photoadsorption* is unknown. In the treatment below, we assume that there is a constant fraction of the cresols adsorbed on the $Ti^{IV}-OH$ surface sites where photooxidation takes place to yield the intermediates (4-MCC, MHQ, and others). Continued reaction of these intermediate products ultimately yields CO_2 and H_2O via ring cleavage and subsequent formation of peroxides, aldehydes, and carboxylates as occurs in the photodegradation of surfactants (38). With our present results, we summarize the photomineralization process by reactions (12) (CR is a cresol):



The rate of formation of MHQ, other intermediates, and CO_2 is then given by (7)

$$\text{Rate} = \frac{k_{12b} K_{CR} [\text{CR}] [\text{site}]_0}{1 + \{(k_{12b} + k_{12c})/k_{12c}\} K_{CR} [\text{CR}]}, \quad (13)$$

where $K_{CR} = \{k_{12a}/(k_{-12a} + k_{12b})\}$ is the photoadsorption coefficient for the cresol. Since

$k_{12b} \sim k_{12c}$ (see Table 4), Rate = $k_{12b} K_{CR} [\text{CR}] [\text{site}]_0 / (1 + 2K_{CR} [\text{CR}])$, which is of a form similar to the LH kinetic rate law. Considering that OH radicals are formed from a light-assisted process (reactions (3) and (6)), their formation and disappearance through back reactions also need to be accounted for in the expression for the overall rate of product formation.

At low radiant power levels, the quantum yield of formation of OH species is $\Phi_{\cdot\text{OH}} = \phi I_a k_6 \tau$, where τ is the lifetime of the valence band holes of the photocatalyst $\{= 1/(k_{\text{rec}} + k_6)\}$. Taking $k_{\text{rec}} > k_6$ (39), $\Phi_{\cdot\text{OH}} = \phi I_a \beta A_p k_6 / k_{\text{rec}}$, where βA_p represents the fraction of the particle surface that is irradiated and A_p is the particle surface area. The overall rate will also depend on the lifetime of the

$\cdot\text{OH}$ radicals $\tau_{\cdot\text{OH}}$. Further modifications must be noted. Water, MHQ, and other intermediates that form in the degradation process can, in principle, compete for the same adsorption sites as the cresols; these will act as inhibitors. We have also noted that molecular O_2 affects the rate of degradation. Thus, the rate of formation of the products become

$$\text{Rate} = \frac{(\phi I_a \beta A_p k_6 \tau_{\cdot\text{OH}} / k_{\text{rec}}) k_{12b} K_{\text{CR}} [\text{CR}] [\text{site}]_0}{\{1 + 2K_{\text{CR}} [\text{CR}] + K_{\text{W}} [\text{H}_2\text{O}] + K_{\text{MHQ}} [\text{MHQ}] + \sum_i K_{\text{Int}} [\text{Int}]_i\}} \cdot \frac{K_{\text{O}_2} [\text{O}_2]}{(1 + K_{\text{O}_2} [\text{O}_2])} \quad (14)$$

Equation (14) has the same analytical form as those reported by Okamoto and co-workers (17) for the photodegradation of phenol and more recently by Turchi and Ollis (29). The latter authors have presented an elegant rigorous treatment of the kinetics involved in the photooxidations of organic substrates on an irradiated semiconductor surface for a variety of conditions: namely, (i) the oxidizing species ($\cdot\text{OH}$) and the organic substrate are both adsorbed on the catalyst's surface, (ii) the $\cdot\text{OH}$ radical migrates to the bulk solution (*free* $\cdot\text{OH}$) and reacts with the substrate in solution, (iii) the surface bound $\cdot\text{OH}$ radical reacts with the bulk solution organic substrate, and (iv) finally the oxidation occurs between a surface adsorbed organic substrate and *free* $\cdot\text{OH}$ radicals in solution. They concluded that the analytical form of the above expression (14), or its equivalent, precludes distinguishing the actual operational mechanism(s) from the LH pathway. Our treatment confirms this conclusion. Details of the photodegradation pathway(s) must be sought experimentally by probing the initial step(s) of the oxidation process (30, 40). Elsewhere, we will present experimental evidence that the $\cdot\text{OH}$ radical cannot migrate significantly to the bulk solution (40) and thereby react with bulk solution substrates.

CONCLUSIONS

The complete photomineralization of *ortho*-, *meta*-, and *para*-cresol to CO_2 and water in air-equilibrated, irradiated TiO_2 suspensions takes place in ~ 7 – 8 hr at pH 3. In excess molecular oxygen, degradation is faster (≤ 2.5 hr). The various experimental factors that can influence the overall rate of degradation have been examined in some detail. Two major intermediates have been identified, 4-methylcatechol and methylhydroquinone; other intermediates also form but were not identified under our experimental conditions. The present work adds another example of the classes of environmental organic contaminants that may be present in wastewaters and which can be degraded effectively by the photocatalytic method employed herein.

ACKNOWLEDGMENTS

Support of our work by the Natural Science and Engineering Research Council of Canada, by the North Atlantic Treaty Organization (NATO Grant CRG-890746), and by the CNR Rome is gratefully acknowledged.

REFERENCES

- Callahan, M. A., Slimak, M., Gbel, N., May, I., Fowler, C., Freed, R., Jennings, P., Dupree, R., Whitmore, F., Maestri, B., Holt, B., and Gould, C., "Water Related Environmental Fate of 129

- Priority Pollutants," United States Environmental Protection Agency, Report EPA-44014-79-029a,b, NTIS, Washington, DC, 1979.
- Dangerous Prop. Ind. Mater. Rep.* **5**, 30 (1985), and references therein.
 - Dangerous Prop. Ind. Mater. Rep.* **6**, 41 (1986), and references therein.
 - Al-Ekabi, H., and Serpone, N., *J. Phys. Chem.* **92**, 5726 (1988). [Part 1]
 - Al-Ekabi, H., Serpone, N., Pelizzetti, E., Minero, C., Fox, M. A., and Draper, R. B., *Langmuir* **5**, 250 (1989). [Part 2]
 - (a) Pelizzetti, E., Minero, C., Maurino, V., Sclafani, A., Hidaka, H., and Serpone, N., *Environ. Sci. Technol.* **23**, 1385 (1989) [Part 3]; (b) Terzian, R., Serpone, N., Minero, C., Pelizzetti, E., and Hidaka, H., *J. Photochem. Photobiol. A Chem.*, in press. [Part 4]
 - Laidler, K. J., "Chemical Kinetics," 3rd ed., pp. 400-406. Harper & Row, New York, 1987.
 - Technical Bulletin No. 56, Degussa Canada Ltd.
 - Borgarello, E., Serpone, N., Barbeni, M., and Pelizzetti, E., *J. Photochem.* **33**, 35 (1986).
 - Pelizzetti, E., Pramauro, E., Minero, C., Serpone, N., and Borgarello, E., in "Photocatalysis and Environment" (M. Schiavello, Ed.), NATO ASI Series, Ser. C237, pp. 468-497. Kluwer, Dordrecht, 1988, and references therein.
 - Serpone, N., Borgarello, A., and Pelizzetti, E., in "Photocatalysis and Environment" (M. Schiavello, Ed.), NATO ASI Series, Ser. C237, pp. 527-565. Kluwer, Dordrecht, 1988, and references therein.
 - See, for example, Grätzel, M., "Heterogeneous Photochemical Electron Transfer," CRC p. 125. Boca Raton, FL, 1989.
 - Harris, D. C., "Quantitative Chemical Analysis," Appendix G. Freeman, New York, 1982.
 - Barbeni, M., Pramauro, E., Pelizzetti, E., Borgarello, E., Grätzel, M., and Serpone, N., *Nouv. J. Chim.* **8**, 550 (1984).
 - Barbeni, M., Pelizzetti, E., Borgarello, E., and Serpone, N., *Chemosphere* **14**, 195 (1985).
 - Okamoto, K., Yamamoto, Y., Tanaka, H., Tanaka, M., and Itaya, A., *Bull. Chem. Soc. Japan* **58**, 2015 (1985).
 - Okamoto, K., Yamamoto, Y., Tanaka, H., and Itaya, A., *Bull. Chem. Soc. Japan* **58**, 2023 (1985).
 - Terzian, R., and Serpone, N.; unpublished observations.
 - (a) Matthews, R. W., *J. Chem. Soc. Faraday Trans. 1* **80**, 457 (1984); (b) *J. Catal.* **97**, 565 (1986); (c) *Water Res.* **20**, 569 (1986); (d) *J. Phys. Chem.* **91**, 3328 (1987); (e) *Sol. Energy* **38**, 405 (1987); (f) *Aust. J. Chem.* **40**, 667 (1987).
 - Izumi, I., Dunn, W. W., Willbourn, K. O., Fran, F. F., and Bard, A. J., *J. Phys. Chem.* **84**, 3207 (1980).
 - Fujihira, M., Satoh, Y., and Osa, T., *Bull. Chem. Soc. Japan* **55**, 666 (1982).
 - Izumi, I., Fran, F. F., and Bard, A. J., *J. Phys. Chem.* **85**, 218 (1981).
 - Cunningham, J., and Srijarani, S., *J. Photochem. Photobiol. A Chem.* **43**, 329 (1988).
 - (a) Ceresa, E. M., Burlamacchi, L., and Visca, M., *J. Mater. Sci.* **18** 289 (1983); (b) Jaeger, C. D., and Bard, A. J., *J. Phys. Chem.* **83**, 3146 (1979); (c) Bolton, J. R., personal communication.
 - Cundall, R. B., Rudham, R., and Salim, M. S., *J. Chem. Soc. Faraday Trans. 1* **72**, 1642 (1976).
 - Harvey, P. R., Rudham, R., and Ward, S., *J. Chem. Soc. Faraday Trans. 1* **79**, 1381 (1983).
 - Herrmann, J.-M., and Pichat, P., *J. Chem. Soc. Faraday Trans. 1* **76**, 1138 (1980).
 - Kormann, C., Bahnemann, D. W., and Hoffmann, M. R., *Environ. Sci. Technol.* **22**, 798 (1988).
 - Turchi, C. S., and Ollis, D. F., *J. Catal.* **122**, 178 (1990).
 - Fox, M. A., in "Proceedings of IPS-8 Solar Energy Conference, Palermo, Italy, July 15-20, 1990."
 - Ref. (7), pp. 278-281.
 - Ref. (7), pp. 379-384.
 - Pichat, P., and Herrmann, J.-M., in "Photocatalysis—Fundamentals and Applications" (N. Serpone and E. Pelizzetti, Eds.), pp. 217-250. Wiley-Interscience, New York, 1989.
 - Al-Ekabi, H., and Serpone, N., in "Photocatalysis—Fundamentals and Applications" (N. Serpone and E. Pelizzetti, Eds.), pp. 457-488. Wiley-Interscience, New York, 1989.
 - Nagao, M., and Suda, Y., *Langmuir* **3**, 786 (1987).
 - (a) Munuera, G., Rives-Arnau, V., and Sancedo, A., *J. Chem. Soc. Faraday Trans. 1* **75**, 736 (1979); (b) Harbour, J. R., and Hair, M. L., *J. Phys. Chem.* **83**, 652 (1979); (c) Howe, R. F., and Grätzel, M., *J. Phys. Chem.* **89**, 4495 (1985); (d) Munuera, G., Gonzalez-Eliphe, A. R., Rives-Arnau, V., Navio, A., Malet, P., Soria, J., Conesa, J. C., and Sanz, J., in "Adsorption and Catalysis on Oxide Surfaces" (M. Che and G. C. Bond, Eds.). Elsevier, Amsterdam, 1985.
 - Howe, R. F., and Grätzel, M., *J. Phys. Chem.* **91**, 3906 (1987).
 - Hidaka, H., Zhao, J., Suenaga, S., Pelizzetti, E., and Serpone, N., submitted for publication.
 - Rothenberger, G., Moser, J., Grätzel, M., Serpone, N., and Sharma, D. K., *J. Amer. Chem. Soc.* **107**, 8054 (1985).
 - Lawless, D., Serpone, N., and Meisel, D., submitted for publication.